

000 001 002 003 004 005 006 007 008 009 010 CellDuality: UNLOCKING BIOLOGICAL REASONING IN LLMS WITH SELF-SUPERVISED RLVR

005
006
007
008
009
010
Anonymous authors
011
012
013
014
015
016
017
018
019
020
021
022
023
024
025
026
027
028
029
030
031
032
033
034
035
036
037
038
039
040
041
042
043
044
045
046
047
048
049
050
051
052
053
Paper under double-blind review
011
012
013
014
015
016
017
018
019
020
021
022
023
024
025
026
027
028
029
030
031
032
033
034
035
036
037
038
039
040
041
042
043
044
045
046
047
048
049
050
051
052
053

ABSTRACT

Developing generalist large language models (LLMs) capable of complex biological reasoning is a central challenge in computational biology. While existing LLMs excel at predictive tasks like cell type annotation and logically-constrained problems, enabling open-ended and mechanistic reasoning remains a challenge. A promising direction is Reinforcement Learning from Verifiable Rewards (RLVR), which has been shown to significantly enhance complex reasoning in general domains like mathematics and code synthesis. However, its application in biology is hindered, as most biological outcomes are non-verifiable. For example, verifying a generated gene sequence is usually infeasible. In this paper, we introduce **CellDuality**, a self-supervised framework that enables LLM agents for robust reasoning in single-cell biology. Our framework is built on the principle of complementary task duality, a self-verification process that leverages a bidirectional reasoning loop. First, the model performs a forward reasoning task by predicting a biological outcome (e.g., a cell’s response to a drug). Then, in a complementary inverse task, it must reason backward from its own prediction to reconstruct the initial conditions (e.g., the original drug perturbation). The fidelity of this reconstruction serves as an intrinsic reward signal, creating a feedback loop that enforces logical and biological consistency. We use these intrinsic rewards to align the base LLM via reinforcement learning, without requiring ground-truth verification labels. We demonstrate that **CellDuality** achieves state-of-the-art performance and provides coherent biological explanations across a diverse suite of single-cell reasoning tasks. Critically, on the challenging out-of-distribution perturbation prediction benchmark, our self-supervised approach significantly outperforms the standard fine-tuning baseline and narrows the performance gap to a supervised RLVR baseline. Our work showcases a new path toward scalable training of biological foundation models.

1 INTRODUCTION

Developing generalist large language models (LLMs) capable of biological reasoning is a central goal of computational biology (Fang et al., 2025b; Istrate et al., 2025; Lotfollahi et al., 2019). This reasoning ability involves inferring complex, mechanistic principles from cellular data (Fang et al., 2025b; Matsumoto et al., 2025). This capability is paramount in single-cell biology, where understanding causal chains, such as how a cell responds to a drug, is key to therapeutic discovery (Fang et al., 2025a). However, achieving robust biological reasoning is fundamentally challenging due to the stochastic nature of cellular systems and the intricate, high-dimensional dependencies between biological entities. This complexity creates a significant hurdle for current methods, especially the foundation models (Hao et al., 2024; Cui et al., 2024), which we categorize into three limitations.

First, most models are optimized for *prediction*, not *mechanistic reasoning*. Architectures like scGPT (Cui et al., 2024) and C2S-Scale (Rizvi et al., 2025) excel at learning correlational patterns for tasks like cell type annotation but are not explicitly trained to generate the coherent, explanatory steps that capture underlying biological pathways. Second, existing reasoning-aware models often operate in *logically-constrained paradigms*. For instance, Cell-01 (Fang et al., 2025b) models a deductive puzzle-solving process rather than the open-ended, hypothesis-driven inquiry of scientific exploration. Finally, there exists a trade-off between *depth and generality*. Specialized models achieve deep reasoning in a single task, while versatile, multi-task agents like InstructCell (Fang

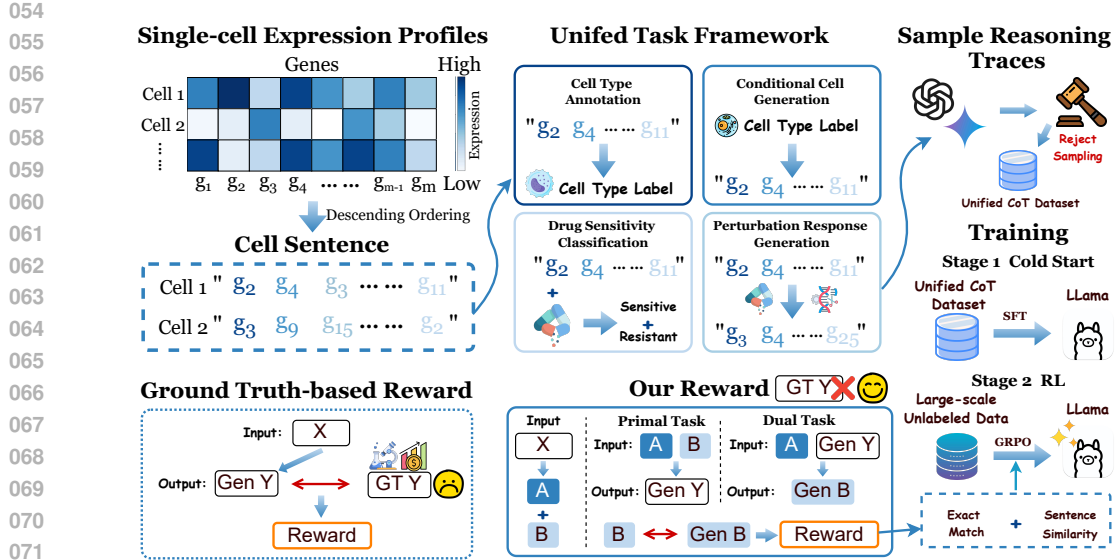


Figure 1: An overview of the **CellDuality** framework. Single-cell expression profiles are first converted into ranked "Cell Sentences," which are inputs to our Unified Task Framework of four reasoning tasks. A high-quality CoT dataset is generated using a teacher model and Reject Sampling. This dataset is used for a Stage 1 SFT cold start of an LLaMA model. The model is then further aligned in Stage 2 via self-supervised RL (GRPO) on large-scale unlabeled data. The core innovation is our duality-based reward mechanism, which replaces the need for external Ground Truth by rewarding the consistency between a Primal Task and its complementary Dual Task.

et al., 2025a) currently lack the same level of mechanistic insight. Therefore, a unifying framework capable of deep reasoning across this diverse task landscape is still an open challenge. Such a framework must achieve generality over two core biological themes: cell identity and cell dynamics.

A promising direction is Reinforcement Learning from Verifiable Rewards (RLVR), a paradigm that has successfully enhanced LLMs' general reasoning ability, such as mathematics and code synthesis (Shao et al., 2024; Rafailov et al., 2023; Lee et al., 2023). However, its application in biology is severely limited because most biological reasoning tasks are inherently non-verifiable. For example, a specific gene sequence output of conditional cell generation has no single correct version for a given cell type, making simple verification infeasible. This data-dependency fundamentally constrains the training of more ambitious, unified models on the open-ended, cause-and-effect scenarios that would foster biological understanding.

To address this challenge, we introduce **CellDuality**, a generalist agent for open-ended biological reasoning. It operates within a unified framework of four core tasks designed to span the fundamental biological themes of cell identity and cell dynamics (details in Sec. 3.1). Crucially, **CellDuality** is trained via a novel self-supervised paradigm built on the principle of *Complementary Task Duality* (She et al., 2025). This framework leverages a bidirectional reasoning loop to generate its own supervisory signals: first, the model performs a forward reasoning task (e.g., predicting a cell's response to a drug); then, in a complementary inverse task, given generated results and known input conditions, it will reason backward to reconstruct the unknown input conditions. The reward is then determined by directly comparing the reconstructed input with the original. This consistency score becomes the intrinsic reward signal, compelling the model to produce forward predictions that are accurate and logically reversible, without needing ground-truth labels for the predictions themselves.

We implement this principle in a two-stage training paradigm. An initial Supervised Fine-Tuning (SFT) stage on a small, curated set of examples, containing both forward and inverse reasoning traces. This stage serves to cold-start the model, teaching it the language and format of biological reasoning. This is followed by a large-scale, self-supervised Reinforcement Learning (RL) stage, where the model is aligned using these intrinsic rewards on vast unlabeled data. This stage refines the model's ability to produce outputs that are not only stylistically correct but also biologically and logically coherent.

108 Empirical evaluations demonstrate that **CellDuality**, despite being trained without any ground-
 109 truth verification during its RL phase, substantially outperforms its SFT-only counterpart. Critically,
 110 on the challenging OOD perturbation benchmark, our self-supervised approach closes XX% of the
 111 performance gap to a fully-supervised RLVR model that was trained with ground-truth rewards.
 112 This showcases the remarkable sample efficiency and generalization capabilities of our framework.
 113 Our main contributions are:

114 • We propose a novel, unified framework that structures complex biological inquiry into four core
 115 reasoning tasks spanning both cell identity and cell dynamics. This provides the first clear
 116 roadmap for developing and evaluating true generalist agents in single-cell biology.
 117 • We introduce the principle of *Complementary Task Duality*, a new mechanism for generating
 118 annotation-free rewards. This framework incentivizes LLMs to learn the intrinsic, causal consis-
 119 tency of biological processes by rewarding the fidelity of a bidirectional reasoning loop, eliminat-
 120 ing the need for ground-truth labels during the RL phase.
 121 • We show empirically that the generalist model significantly outperforms standard SFT baselines
 122 and narrows the performance gap to a fully-supervised oracle model on the challenging out-of-
 123 distribution perturbation prediction benchmark.

125 2 RELATED WORK

127 **Foundation Models in Single-Cell Biology.** Foundation models are revolutionizing single-cell bi-
 128 ology by learning representations from massive transcriptomic data (Cui et al., 2024; Theodoris
 129 et al., 2023). The field has rapidly progressed from models focused on predictive tasks, such as
 130 scGPT (Cui et al., 2024) for annotation and C2S-Scale (Rizvi et al., 2025) for multi-task general-
 131 ity, to those attempting explicit reasoning. However, these reasoning-aware models often operate
 132 in narrow paradigms; for instance, Cell-o1 (Fang et al., 2025b) frames reasoning as a logically-
 133 constrained puzzle, while agentic frameworks like ESCARGOT (Matsumoto et al., 2025) rely on
 134 external knowledge graphs. A key challenge remains in developing a single, generalist agent that
 135 can perform open-ended, mechanistic reasoning directly from cellular data. Our work addresses this
 136 gap, aiming for the generality of models like InstructCell (Fang et al., 2025a) but with a training
 137 objective that explicitly fosters deep, intrinsic reasoning.

138 **Reinforcement Learning from Verifiable Rewards.** Reinforcement learning is increasingly used
 139 to refine LLMs beyond standard SFT, with paradigms evolving to reduce reliance on external super-
 140 vision (Ouyang et al., 2022; Shao et al., 2024). A particularly scalable paradigm is Reinforcement
 141 Learning from Verifiable Rewards (RLVR), which replaces subjective feedback (Bai et al., 2022)
 142 with objective, ground-truth-based rewards from deterministic verifiers (Shao et al., 2024). How-
 143 ever, the prerequisite of a verifiable output severely limits RLVR’s application in biology, where
 144 outcomes are inherently stochastic. Recent work has sought to address this by generating self-
 145 supervised rewards through task duality. For instance, the DuPO (She et al., 2025) framework
 146 introduced a generalized duality for non-invertible tasks, such as mathematical reasoning, by recon-
 147 structing input components to create a reward signal. Building upon this direction, our work adapts
 148 this principle to the unique challenges of biology. We introduce Complementary Task Duality to
 149 generate intrinsic, self-verifiable rewards from the internal consistency of cellular processes, thus
 150 extending the RLVR paradigm to the non-verifiable biological domain.

151 3 METHODOLOGY

153 This section delineates the methodology for training our single-cell biological reasoning model. An
 154 overview of our entire framework is presented in Figure 1. We first define the concepts and the uni-
 155 fied task framework. We then introduce the generalized framework for self-supervision. Finally, we
 156 detail our training pipeline: an initial cold start stage, followed by a self-supervised Reinforcement
 157 Learning stage that uses our duality principle to enhance the model for deeper reasoning.

158 3.1 PRELIMINARIES AND A UNIFIED TASK FRAMEWORK

159 We denote the LLM policy as π_θ , parameterized by θ . Let \mathcal{V} be the global vocabulary of all consid-
 160 ered gene names. Our work addresses a unified set of four core single-cell reasoning tasks, structured

162
163
164
165
166
167
168
169
170
171
172
173
174
175
176
177
178
179
180
181
182
183
184
185
186
187
188
189
190
191
192
193
194
195
196
197
198
199
200
201
202
203
204
205
206
207
208
209
210
211
212
213
214
215
Table 1: The Unified Task Framework for Single-Cell Reasoning.

Theme	Classification Tasks	Generative Tasks
Cell Identity	Cell Type Annotation (Input: Cell, Output: Label)	Conditional Cell Generation (Input: Label, Output: Cell)
Cell Dynamics	Drug Sensitivity Prediction (Input: Cell + Drug, Output: Label)	Perturbation Response Generation (Input: Cell + Drug, Output: New Cell)

into a 2×2 matrix spanning two fundamental biological themes: *Cell Identity* and *Cell Dynamics*. The core data structures for these tasks are defined as follows:

- **Cell Representation:** A cell $\mathbf{c} = \{g_1, g_2, \dots, g_K\}$ is represented as an descending order sequence of its top K expressed genes, where each gene $g_i \in \mathcal{V}$.
- **Perturbation:** A perturbation \mathbf{p} is a structured tuple describing an intervention, e.g., $\mathbf{p} = \{\text{operation}, \text{target}\}$, where $\text{operation} \in \{\text{knockdown}, \text{overexpression}\}$ and $\text{target} \in \mathcal{V}$.
- **Cell Type and Sensitivity Labels:** A cell type t , is a categorical label from a predefined set \mathcal{T} . Similarly, a drug sensitivity label, s , is a categorical label from a set \mathcal{S} .

All inputs to the LLM are constructed as textual prompts \mathbf{x} that combine these components. The model’s output is a textual response \mathbf{y} , generated autoregressively according to the policy $\mathbf{y} \sim \pi_\theta(\cdot | \mathbf{x})$. A response may include a reasoning trace \mathbf{z} and a final answer \mathbf{a} , i.e., $\mathbf{y} = \{\mathbf{z}, \mathbf{a}\}$.

3.2 THE PRINCIPLE OF COMPLEMENTARY TASK DUALITY

A primary obstacle to applying Reinforcement Learning (RL) to the four tasks defined above is the absence of a scalable reward source. In single-cell biology, obtaining ground-truth signals from experiments is prohibitively expensive and slow. Our work is motivated by a **central question**: Can we generate a reliable, intrinsic reward signal directly from the structure of these biological problems themselves, thus enabling RL without external supervision?

To achieve this, inspired by (She et al., 2025), we introduce a self-supervised reward generation framework. The core idea is to reframe a single biological question into a pair of mutually-verifying tasks, a primal task and a complementary dual task. This creates an internal logic loop that the model must satisfy, providing a natural source for an RL reward.

Definition 3.1 (Complementary Task Duality). Let the input space \mathcal{X} of a primal task \mathcal{T}_p be decomposed into disjoint subspaces: \mathcal{X}_k (known components) and \mathcal{X}_u (unknown components), such that $\mathcal{X} = \mathcal{X}_k \cup \mathcal{X}_u$. The *primal task* \mathcal{T}_p is a mapping from $\mathcal{T}_p : \mathcal{X} \rightarrow \mathcal{Y}$. Its *complementary dual task* \mathcal{T}_{cd} is a mapping that leverages the primal output \mathbf{y} and the known component \mathbf{x}_k to reconstruct the unknown component $\hat{\mathbf{x}}_u$:

$$\mathcal{T}_{cd} : (\mathbf{y}, \mathbf{x}_k) \mapsto \hat{\mathbf{x}}_u.$$

Pair $(\mathcal{T}_p, \mathcal{T}_{cd})$ forms a *generalized dual pair* if it satisfies the *complementary consistency principle*:

$$\forall \mathbf{x} \in \mathcal{X}, \mathbf{y} = \mathcal{T}_p(\mathbf{x}) : d(\mathbf{x}_u, \mathcal{T}_{cd}(\mathbf{y}, \mathbf{x}_k)) \leq \epsilon,$$

where $d(\cdot, \cdot) : \mathcal{X}_u \times \mathcal{X}_u$ is a domain-specific distance metric, and $\epsilon \geq 0$ is a tolerance threshold.

The power of this framework lies in its ability to transform an unsupervised problem into a self-verifying one. The consistency principle defined above provides the mechanism to generate rewards: the fidelity of the dual task’s reconstruction, $d(\mathbf{x}_u, \hat{\mathbf{x}}_u)$, serves as a direct, intrinsic measure of the logical and biological coherence of the primal task’s output \mathbf{y} . This approach elegantly sidesteps the challenges of classical dual learning (irreversibility and asymmetry) by leveraging the known component \mathbf{x}_k as a contextual anchor, ensuring the dual task is well-posed.

3.3 TRAINING STAGE 1: SUPERVISED FINE-TUNING FOR CAPABILITY COLD-START

Before RL Training, we first initialize the base LLM with foundational biological knowledge and reasoning patterns through Supervised Fine-Tuning (SFT). This essential cold-start phase ensures the model can effectively engage with the complex, self-supervised tasks in the subsequent alignment stage. The process involves two key steps: generating a high-quality Chain-of-Thought dataset, and then using it to train the model.

216
217

3.3.1 CHAIN-OF-THOUGHT REASONING DATASET GENERATION

218
219
220
221
222

We construct a comprehensive SFT dataset, \mathcal{D}_{SFT} , by leveraging powerful teacher models (e.g., GPT-4o, Gemini 2.5 Pro) to generate Chain-of-Thought (CoT) reasoning traces. A critical aspect of our approach is that \mathcal{D}_{SFT} must equip our model with capabilities for both the primal (forward) reasoning and the complementary dual (inverse) reasoning required in our RL stage. Therefore, we generate and curate distinct data subsets for each direction.

223
224
225
226
227

Primal Task SFT Data. For each of our four core tasks, we generate primal task data. Given an input prompt \mathbf{x}_i , we prompt a teacher model π_{teacher} to generate N candidate responses $\{\mathbf{y}_{i,k} = (\mathbf{z}_{i,k}, \mathbf{a}_{i,k})\}_{k=1}^N$. We then apply task-specific filtering to select high-quality instances for our primal SFT set, $\mathcal{D}_{\text{SFT}}^{\text{primal}}$.

228
229
230
231

- **For Classification Tasks (Annotation & Sensitivity):** We use a strict *Rejection Sampling* protocol. A candidate $\mathbf{y}_{i,k}$ is accepted if its final answer $\mathbf{a}_{i,k}$ exactly matches the ground-truth label \mathbf{a}_i^* . We define an indicator for correctness as $\epsilon_{i,k} = \mathbb{I}(\mathbf{a}_{i,k} = \mathbf{a}_i^*)$. The accepted set for prompt \mathbf{x}_i is $\{\mathbf{y}_{i,k} | \epsilon_{i,k} = 1\}$. This ensures all training examples are factually correct.

232
233
234
235
236
237
238
239

- **For Generative Tasks (Cell & Response Generation):** As no single, unique ground-truth sequence exists for these tasks, a simple exact match is infeasible. Instead, we adopt a *Rank-Aware Filtering* protocol. For each prompt \mathbf{x}_i with a corresponding ground-truth cell sequence \mathbf{a}_i^* , the teacher model generates a candidate response $(\mathbf{z}_i, \mathbf{a}_i)$. The candidate is accepted into \mathcal{D}_{SFT} only if the generated cell sequence \mathbf{a}_i demonstrates high fidelity to the ground truth in terms of both gene overlap and expression ranking. We quantify this using our proposed Rank-Weighted Jaccard Similarity metric (detailed in Appendix A). A candidate is accepted only if its similarity score exceeds a predefined threshold.

240
241
242
243

Dual Task SFT Data. To explicitly teach the model the inverse reasoning required for our duality framework, we construct a corresponding dual task SFT set, $\mathcal{D}_{\text{SFT}}^{\text{dual}}$. For each instance in our curated primal set, we formulate its complementary dual problem.

244
245
246

- For a primal instance $(\mathbf{x} = (\mathbf{x}_k, \mathbf{x}_u), \mathbf{y}^*)$, we construct a dual prompt $\mathbf{x}_{\text{dual}} = (\mathbf{y}^*, \mathbf{x}_k)$. The ground-truth answer for this dual task is the original unknown component, $\mathbf{y}_{\text{dual}}^* = \mathbf{x}_u$.
- For example, for a perturbation response instance where $\mathbf{x}_k = \mathbf{c}_{\text{pre}}$, $\mathbf{x}_u = \mathbf{p}$, and $\mathbf{y}^* = \mathbf{c}_{\text{post}}^*$, the dual SFT sample would be: prompt $(\mathbf{c}_{\text{post}}^*, \mathbf{c}_{\text{pre}})$ paired with the ground-truth answer \mathbf{p} .

249
250
251
252

The teacher model is then prompted to generate CoT reasoning for these dual problems. The final SFT dataset is the union $\mathcal{D}_{\text{SFT}} = \mathcal{D}_{\text{SFT}}^{\text{primal}} \cup \mathcal{D}_{\text{SFT}}^{\text{dual}}$. This hybrid strategy ensures the model is proficient in both forward and inverse reasoning before entering the RL stage.

253
254
255

3.3.2 SUPERVISED FINE-TUNING OBJECTIVE

256
257

The model is then trained on \mathcal{D}_{SFT} by minimizing the standard negative log-likelihood loss $\mathcal{L}_{\text{SFT}}(\theta)$ over the complete reasoning trajectories:

258
259
260
261

$$\mathcal{L}_{\text{SFT}}(\theta) = -\mathbb{E}_{(\mathbf{x}_i, \mathbf{y}_i^*) \sim \mathcal{D}_{\text{SFT}}} \left[\sum_{j=1}^{|\mathbf{y}_i^*|} \log \pi_{\theta}(y_{i,j}^* | \mathbf{x}_i, \mathbf{y}_{i,<j}^*) \right]. \quad (1)$$

262
263

The resulting model, π_{SFT} , possesses the baseline capabilities required for the subsequent self-supervised alignment.

264
265
266

3.4 STAGE 2: SELF-SUPERVISED DUALITY-GUIDED REINFORCEMENT LEARNING

267
268
269

This stage constitutes the core of our self-supervised methodology. We refine the capabilities of the SFT-initialized model, π_{SFT} , by aligning it with the principle of complementary consistency. This is achieved through a Reinforcement Learning (RL) framework that operates on a large, unlabeled dataset \mathcal{D}_{RL} and is guided by intrinsic rewards, eliminating the need for any ground-truth data.

270 3.4.1 SELF-SUPERVISED REWARD GENERATION
271

272 The cornerstone of our alignment stage is the generation of intrinsic rewards derived from the
273 complementary duality principle. For any prompt $\mathbf{x} = (\mathbf{x}_k, \mathbf{x}_u)$ and a model-generated primal output \mathbf{y} ,
274 we compute a reward by executing the complementary dual task and measuring its reconstruction
275 fidelity. We employ two types of rewards, categorical and sequence-based, tailored to the nature of
276 our core tasks.

277 **Categorical Rewards from Inverse Task Consistency.** For generative tasks such as Perturbation
278 Response Generation and Conditional Cell Generation, the duality provides a clean, categorical
279 reward signal. In both cases, the primal task generates a high-dimensional cell sequence (\mathbf{c}_{post} or \mathbf{c}),
280 and the complementary dual task attempts to reconstruct a categorical input label (the sensitivity \mathbf{s}
281 or the cell type t). The reward is a binary signal based on the exact reconstruction of this label:

$$283 \quad r(\mathbf{y}|\mathbf{x}) = \mathbb{I}(\hat{\mathbf{x}}_u = \mathbf{x}_u), \quad (2)$$

284 where \mathbf{x}_u is the original categorical input (e.g., t) and $\hat{\mathbf{x}}_u$ is its reconstruction (e.g., \hat{t}). This
285 reward directly measures the logical consistency of the generated output: a biologically plausible cell
286 sequence should unambiguously encode the conditions that generated it.

287 **Continuous Rewards from Conditional Inpainting.** For classification tasks such as Cell Type
288 Annotation and Drug Sensitivity Prediction, where the primal output is a low-information label, we
289 design a reward based on a conditional gene inpainting objective. Here, the input cell sequence
290 is artificially decomposed into an observed part \mathbf{c}_{obs} and a hidden part \mathbf{c}_{hid} , which serves as the
291 unknown component \mathbf{x}_u . The dual task is to reconstruct $\hat{\mathbf{c}}_{\text{hid}}$ conditioned on both the observed genes
292 \mathbf{c}_{obs} and the model’s predicted primal label (\hat{t} or \hat{s}). The reward is a continuous score reflecting
293 the quality of this reconstruction: $r(\hat{t}|\mathbf{c}) = \text{RWJS}(\mathbf{c}_{\text{hid}}, \hat{\mathbf{c}}_{\text{hid}})$. Here, we use Rank-Weighted Jaccard
294 Similarity (detailed in Appendix. A) to measure the similarity between the original hidden genes
295 and the reconstructed ones. This reward incentivizes the model to base its classification on a deep
296 understanding of the cell’s underlying gene signature, as a correct label should provide the necessary
297 context for accurate gene inpainting.

300 3.4.2 POLICY OPTIMIZATION WITH GRPO
301

302 We optimize the policy π_θ to maximize the expected self-supervised reward $\mathcal{J}(\theta) =$
303 $\mathbb{E}_{\mathbf{x} \sim \mathcal{D}_{\text{RL}}} [r(\mathbf{y}|\mathbf{x})]$. We employ Group Relative Policy Optimization (GRPO), a memory-efficient and
304 stable critic-free RL algorithm. The optimization follows an iterative, online process: for each
305 prompt, the current policy π_θ generates a group of G candidate responses, each of which is then
306 assigned a self-supervised reward based on its dual-task performance. This group of responses and
307 rewards is then used to update the policy as follows.

308 **Advantage Estimation.** For each prompt, after generating a group of G responses and their cor-
309 responding rewards $\{r_k\}_{k=1}^G$, we compute the advantage for each candidate. This is achieved by
310 normalizing the rewards relative to the group’s performance, which serves as an empirical baseline,
311 thus obviating the need for a separate value function:

$$312 \quad A_k = \frac{r_k - \text{mean}(\{r_j\}_{j=1}^G)}{\text{std}(\{r_j\}_{j=1}^G) + \epsilon}. \quad (3)$$

315 **Objective Function.** The policy is updated by maximizing the GRPO objective, which includes a
316 clipped surrogate objective to stabilize training and a KL penalty to prevent large deviations from a
317 reference policy π_{ref} (typically the initial SFT model π_{SFT}):

$$319 \quad \mathcal{J}_{\text{GRPO}}(\theta) = \mathbb{E} [\min(\rho_t(\theta)A_t, \text{clip}(\rho_t(\theta), 1 - \epsilon_c, 1 + \epsilon_c)A_t) - \beta D_{\text{KL}}(\pi_\theta \parallel \pi_{\text{ref}})], \quad (4)$$

320 where $\rho_t(\theta) = \pi_\theta(y_t|x)/\pi_{\theta_{\text{old}}}(y_t|x)$ is the probability ratio, A_t is the advantage at token t (in our
321 case, A_k is applied to all tokens of response k), ϵ_c is the clipping ratio, and β is the KL coeffi-
322 cient. This iterative, multi-task training process progressively refines the model’s ability to generate
323 biologically coherent and logically consistent responses.

324

4 EXPERIMENT

325

4.1 EXPERIMENTAL SETUP

328 **Tasks and Datasets.** Our evaluation is centered around the four core single-cell reasoning tasks
 329 introduced in our framework. To ensure fair and direct comparison with state-of-the-art models, we
 330 adopt the exact datasets and train/test splits used in seminal works, including C2S-Scale (Rizvi et al.,
 331 2025) and InstructCell (Fang et al., 2025a). Our training strategy involves fine-tuning a single base
 332 model on a designated primary training set for each task theme, and then evaluating its performance
 333 on both in-distribution (ID) and out-of-distribution (OOD) test sets.

334

- **Cell Identity Tasks (Annotation & Generation):**

- **Training Dataset:** To build a robust generalist model for cell identity, we construct a mixed training dataset by combining the training splits of four diverse public benchmarks: He-2020-Liver (He et al., 2020), Segerstolpe-2016 (Segerstolpe et al., 2016), Xin-2016 (Xin et al., 2016), and Human Immune Tissue Dataset (Domínguez Conde et al., 2022). This mixed dataset serves as the sole source of supervision for our model on all identity tasks.
- **ID Test Set:** For the cell type annotation task, we use the held-out test splits of the three datasets included in our training mix (He-2020-Liver, Segerstolpe-2016, Xin-2016). For cell generation, we use the held-out test splits of Human Immune Datasets.
- **OOD Test Set:** We use two datasets entirely unseen during training: Ma-2020 (Ma et al., 2020) and Bastidas-Ponce-2019 (Bastidas-Ponce et al., 2019).

345

- **Cell Dynamics Tasks (Sensitivity Prediction & Response Generation):**

- **Training Dataset:** We construct a comprehensive mixed training dataset by combining three distinct perturbation benchmarks: the L1000 dataset (Subramanian et al., 2017), which covers two human drug response datasets, GSE149383 (Lung) (Aissa et al., 2021) and GSE117872 (Oral Cavity) (Sharma et al., 2018). This diverse dataset, containing examples for both response generation and sensitivity classification, serves as the sole source of supervision for our model on all dynamics-related tasks.
- **ID Test Sets:** The held-out test splits of the two datasets explicitly included for the classification task: GSE149383 and GSE117872.
- **OOD Test Sets:** We use two benchmarks entirely unseen during training. For cross-species classification, we use the complete GSE110894 (Mouse Bone Marrow) dataset (Bell et al., 2019). For generative causal reasoning, we use the OOD splits of the sci-Plex3 Human Perturbation dataset (Srivatsan et al., 2020).

359

Evaluation Metrics.

- For Classification Tasks (Cell Type Annotation, Drug Sensitivity): We report *Accuracy* as the primary metric. We also include the *Macro F1-score* to account for class imbalance.
- For Generative Tasks (Conditional Generation, Perturbation Response): For Perturbation Response Generation, we follow C2S-Scale (Rizvi et al., 2025) and report distribution-based metrics (scFID and MMD) calculated in a pre-trained embedding space (scGPT (Cui et al., 2024)) to assess the quality and realism of generated cell populations. For Conditional Cell Generation, we follow Cell2Sentence (LeVine et al., 2024) and report Gromov-Wasserstein (GW) Distance and k-NN Accuracy. The k-NN classifier is evaluated with multiple neighbor values ($k \in \{3, 5, 10, 25\}$).

369 **Baseline Models.** We benchmark **CellDuality** against a comprehensive set of state-of-the-art
 370 models, with all performance metrics cited directly from the original publications for fair com-
 371 parison. For classification tasks (Annotation and Sensitivity), we compare against domain-specific
 372 foundation models such as **scGPT** (Cui et al., 2024) and **Geneformer** (Theodoris et al., 2023), as
 373 well as LLM-based agents like **InstructCell** (Fang et al., 2025a). For generative tasks (Cell and
 374 Response Generation), baselines include specialized generative models like **scGen** (Lotfollahi et al.,
 375 2019) and **scDiffusion** (Luo et al., 2024), and the powerful LLM-based framework **C2S-Scale** (Rizvi
 376 et al., 2025).

377 **Implementation Details.** Our **CellDuality** model is based on the Llama-3.2-3B architecture. The
 SFT stage is conducted for 3 epochs with a learning rate of $1e - 5$. The subsequent self-supervised

378
 379 Table 2: Performance comparison on the Cell Type Annotation task. Baselines are trained on each
 380 dataset individually. We report Accuracy (Acc.) and Macro F1-score (F1) for all five benchmarks,
 381 differentiating between ID and OOD evaluation for our model.

Model	In-Distribution (ID) Evaluation						Out-of-Distribution (OOD) Evaluation			
	He-2020-Liver		Segerstolpe-2016		Xin-2016		Ma-2020		Bastidas-Ponce-2019	
	Acc. (%)	F1 (%)	Acc. (%)	F1 (%)	Acc. (%)	F1 (%)	Acc. (%)	F1 (%)	Acc. (%)	F1 (%)
scBERT	95.28	94.08	99.52	99.64	99.25	98.79	82.92	81.73	86.67	79.60
scGPT	94.88	91.75	98.09	97.82	99.10	98.40	82.84	79.40	91.43	87.01
Geneformer	96.06	92.57	99.52	99.49	99.70	99.39	85.79	84.89	88.50	83.81
Cell2Sentence	94.88	94.42	99.52	99.64	99.35	98.77	82.40	81.05	80.59	76.82
InstructCell-instruct	96.06	95.24	100.00	100.00	99.30	98.89	85.59	84.56	91.10	88.69
CellDuality (SFT-only)	94.83 ± 0.21	94.67 ± 0.18	98.76 ± 0.08	98.73 ± 0.09	99.45 ± 0.12	99.01 ± 0.15	80.22 ± 0.34	74.95 ± 0.41	72.87 ± 0.28	57.24 ± 0.33
CellDuality	96.34 ± 0.19	95.41 ± 0.16	99.81 ± 0.07	99.78 ± 0.08	99.52 ± 0.11	99.08 ± 0.13	82.03 ± 0.32	81.78 ± 0.39	88.45 ± 0.26	78.12 ± 0.31

388
 389 Table 3: Performance comparison on the Drug Sensitivity Classification task. Baselines are trained
 390 on each dataset individually. We report Accuracy (Acc.) and Macro F1-score (F1).

Model	In-Distribution (ID) Evaluation				Out-of-Distribution (OOD) Evaluation		
	GSE149383 (Human Lung)		GSE117872 (Human Oral)		GSE110894 (Mouse Bone)		
	Acc. (%)	F1 (%)	Acc. (%)	F1 (%)	Acc. (%)	F1 (%)	
scBERT	99.56	99.56	95.42	96.01	95.80	95.79	
scGPT	97.79	97.79	82.44	84.76	95.80	95.79	
Geneformer	98.23	98.23	94.66	95.27	93.01	92.91	
Cell2Sentence	93.36	93.36	90.84	90.72	95.10	95.08	
InstructCell-instruct	97.35	97.34	100.00	100.00	97.20	97.19	
CellDuality (SFT-only)	98.91 ± 0.15	98.89 ± 0.16	96.78 ± 0.22	97.12 ± 0.19	96.45 ± 0.18	96.42 ± 0.20	
CellDuality	99.12 ± 0.13	99.10 ± 0.14	97.23 ± 0.20	97.58 ± 0.17	96.12 ± 0.21	96.08 ± 0.23	

400
 401 Table 4: Performance on Perturbation Response Generation (sci-Plex3 benchmark). Our model was
 402 trained on a separate perturbation dataset, while baselines were trained on the in-distribution splits
 403 of sci-Plex3. Lower scores are better for distribution-based metrics.

Model	Supervision Type	scFID (↓)	MMD (↓)	Wasserstein (↓)
scGen	Supervised	0.95	1.05	0.98
CellOT	Supervised	0.88	1.03	0.95
scGPT	Supervised	0.29	0.42	0.54
C2S-Scale 1B (SFT)	Supervised	0.02	0.01	0.21
C2S-Scale (GRPO w/ GT)	Ground-Truth RL	0.02	0.01	0.21
CellDuality (SFT-only)	Supervised	0.045 ± 0.003	0.028 ± 0.002	0.267 ± 0.012
CellDuality	Self-Supervised	0.038 ± 0.002	0.019 ± 0.001	0.245 ± 0.011

412
 413 RL alignment is performed using GRPO with a group size of $G = 8$. All experiments are conducted
 414 on 8x A6000 GPUs. All our scores are shown as mean \pm std over 5 runs.

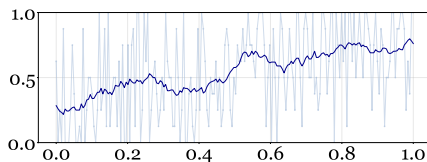
4.2 MAIN RESULTS

418
 419 Across all four reasoning tasks, our self-supervised framework, **Cell-Duality**, demonstrates
 420 highly competitive performance against a wide range of state-of-the-art baselines. As detailed in Ta-
 421 bles 2 through 5, our generalist model, trained on mixed datasets, consistently matches or surpasses
 422 specialist models that were trained on individual benchmarks. This is particularly evident in the
 423 classification tasks (Cell Type Annotation and Drug Sensitivity), where **CellDuality** shows robust
 424 generalization to out-of-distribution and even cross-species datasets.

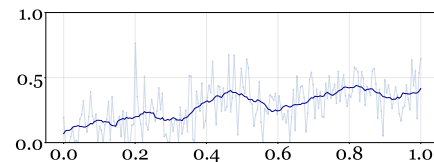
425
 426 The most significant impact of our self-supervised approach is observed in the generative tasks
 427 requiring deep causal reasoning. For Perturbation Response Generation, the duality-guided RL stage
 428 provides a substantial performance boost over the already strong SFT baseline. Critically, our self-
 429 supervised model successfully narrows the performance gap to a fully-supervised oracle that requires
 430 ground-truth labels for alignment, proving the efficacy of our annotation-free strategy. While our
 431 model also demonstrates strong performance on Conditional Cell Generation by outperforming most
 432 classical and deep learning-based generative models, its primary strength lies in its ability to learn the
 433 intrinsic, mechanistic consistency of biological processes, showcasing a new path toward scalable
 434 and robust scientific reasoning agents.

432
 433 Table 5: Performance on Conditional Cell Generation on the Human Immune dataset (In-
 434 Distribution). Baseline results are cited from Cell2Sentence (LeVine et al., 2024). k-NN Accuracy
 435 is reported for multiple values of k.

436 437 Model	438 439 440 441 442 443 k-NN Accuracy (%) ↑				444 445 446 447 448 449 GW Distance (↓)
	444 445 k=3	446 447 k=5	448 449 k=10	450 451 k=25	
scVI	24.36 \pm 0.0062	24.00 \pm 0.0064	24.25 \pm 0.0034	23.48 \pm 0.0032	302.13 \pm 0.9338
scGen	23.76 \pm 0.0112	23.30 \pm 0.0093	23.77 \pm 0.0053	23.35 \pm 0.0041	315.95 \pm 1.2431
scDiffusion	23.35 \pm 0.0125	22.88 \pm 0.0111	23.68 \pm 0.0067	23.06 \pm 0.0049	72.02 \pm 0.3937
scGPT	18.38 \pm 0.0086	17.88 \pm 0.0169	18.11 \pm 0.0149	18.82 \pm 0.0071	2989.81 \pm 4.9229
Cell2Sentence-160M	25.88 \pm 0.0061	25.65 \pm 0.0060	27.46 \pm 0.0073	27.15 \pm 0.0070	54.30 \pm 0.3410
CellDuality (SFT-only)	24.92 \pm 0.0058	24.71 \pm 0.0055	25.83 \pm 0.0062	25.49 \pm 0.0059	63.87 \pm 0.0421
CellDuality	26.34 \pm 0.0056	25.92 \pm 0.0053	26.21 \pm 0.0060	25.98 \pm 0.0057	61.45 \pm 0.0408



(a) Categorical Reward (Generative Tasks)



(b) Continuous Reward (Classification Tasks)

450
 451 Figure 2: **Training dynamics of self-supervised rewards during the RL alignment stage.** The
 452 plots show the moving average of (a) the categorical accuracy-based reward for generative tasks and
 453 (b) the continuous RWJS-based reward for classification tasks.

454 Table 6: Core ablation study comparing Self-Supervised RL against a Ground-Truth Supervised
 455 oracle. All models are initialized from the same SFT checkpoint and evaluated on their respective
 456 **in-distribution (ID)** test sets.

457 458 Method Configuration	459 He-2020-Liver		460 GSE149383 (Lung)		461 sci-Plex3	
	462 Acc. (↑)	463 F1 (↑)	464 Acc. (↑)	465 F1 (↑)	466 scFID (↓)	467 MMD (↓)
Llama-3.2-3B-Instruct	22.45 \pm 1.23	52.82 \pm 1.45	29.67 \pm 0.89	61.34 \pm 1.12	-	-
SFT-only	95.83 \pm 0.21	94.67 \pm 0.18	98.91 \pm 0.15	98.89 \pm 0.16	0.045 \pm 0.003	0.028 \pm 0.002
RL with Ground-Truth	97.21 \pm 0.16	94.85 \pm 0.14	99.34 \pm 0.12	99.31 \pm 0.13	0.025 \pm 0.001	0.012 \pm 0.001
Ours (Self-Supervised RL)	96.34 \pm 0.19	95.41 \pm 0.16	99.12 \pm 0.13	99.10 \pm 0.14	0.038 \pm 0.002	0.019 \pm 0.001

468 4.3 ABLATION STUDY

469 **Self-Supervised vs. Ground-Truth Supervised RL** To rigorously quantify the efficacy of our self-
 470 supervised alignment strategy, we conduct a head-to-head comparison against a standard supervised
 471 RL approach. We evaluate three key models on their respective in-distribution test sets: (1) the
 472 SFT-only baseline, (2) a supervised RL oracle trained with ground-truth rewards, and (3) our self-
 473 supervised **CellDuality** model. As shown in Table 6, our self-supervised RL approach consistently
 474 and significantly boosts performance over the SFT-only baseline across all tasks. Critically, our
 475 annotation-free method substantially narrows the performance gap to the fully-supervised oracle,
 476 and even surpasses the oracle’s Macro F1-score on the He-2020-Liver annotation task, suggesting it
 477 learns more robust decision boundaries.

478 5 CONCLUSION

479 We introduced **CellDuality**, a generalist agent that learns complex biological reasoning through
 480 a novel self-supervised framework. Our core contribution, the principle of complementary task
 481 duality, enables reinforcement learning alignment on non-verifiable single-cell tasks by generating
 482 intrinsic rewards from a bidirectional reasoning loop. Trained via our sample-efficient, two-stage
 483 paradigm, **CellDuality** achieves state-of-the-art performance across four distinct reasoning tasks,
 484 providing coherent biological explanations. Critically, our self-supervised approach demonstrates
 485 its efficacy by narrowing the performance gap to a supervised RLVR baseline. This work presents a
 486 significant step toward scalable foundation models in biology, offering a new paradigm that learns
 487 to reason from the intrinsic logical structure of scientific problems, rather than from external labels.

486 ETHICS STATEMENT
487488 We adhere to the ICLR Code of Ethics. No private, sensitive, or personally identifiable data are in-
489 volved. Our work does not raise foreseeable ethical concerns or produce harmful societal outcomes.
490491 REPRODUCIBILITY STATEMENT
492493 Reproducibility is central to our work. All datasets used in our experiments are standard benchmarks
494 that are publicly available. We provide full details of the training setup, model architectures, and
495 evaluation metrics in the main paper and appendix. Upon acceptance, we will release our codebase,
496 including scripts for preprocessing, training, and evaluation, along with configuration files and doc-
497 umentation to facilitate exact reproduction of our results. Random seeds and hyperparameters will
498 also be included to further ensure reproducibility.
499500 REFERENCES
501

502 Alexandre F Aissa, Abul BMMK Islam, Majd M Ariss, Cammille C Go, Alexandra E Rader,
503 Ryan D Conrady, Alexa M Gajda, Carlota Rubio-Perez, Klara Valyi-Nagy, Mary Pasquinelli,
504 et al. Single-cell transcriptional changes associated with drug tolerance and response to combi-
505 nation therapies in cancer. *Nature communications*, 12(1):1628, 2021.

506 Yuntao Bai, Saurav Kadavath, Sandipan Kundu, Amanda Askell, Jackson Kernion, Andy Jones,
507 Anna Chen, Anna Goldie, Azalia Mirhoseini, Cameron McKinnon, et al. Constitutional ai: Harm-
508 lessness from ai feedback. *arXiv preprint arXiv:2212.08073*, 2022.

509 Aimée Bastidas-Ponce, Sophie Tritschler, Leander Dony, Katharina Scheibner, Marta Tarquis-
510 Medina, Ciro Salinno, Silvia Schirge, Ingo Burtscher, Anika Böttcher, Fabian J Theis, et al.
511 Comprehensive single cell mrna profiling reveals a detailed roadmap for pancreatic endocrino-
512 genesis. *Development*, 146(12):dev173849, 2019.

513 Charles C Bell, Katie A Fennell, Yih-Chih Chan, Florian Rambow, Miriam M Yeung, Dane Vas-
514 siliadis, Luis Lara, Paul Yeh, Luciano G Martelotto, Aljosja Rogiers, et al. Targeting enhancer
515 switching overcomes non-genetic drug resistance in acute myeloid leukaemia. *Nature communi-
516 cations*, 10(1):2723, 2019.

517 Haotian Cui, Chloe Wang, Hassaan Maan, Kuan Pang, Fengning Luo, Nan Duan, and Bo Wang.
518 scgpt: toward building a foundation model for single-cell multi-omics using generative ai. *Nature
519 Methods*, pp. 1–11, 2024.

520 C Domínguez Conde, Chao Xu, Louie B Jarvis, Daniel B Rainbow, Sara B Wells, Tamir Gomes,
521 SK Howlett, O Suchanek, K Polanski, HW King, et al. Cross-tissue immune cell analysis reveals
522 tissue-specific features in humans. *Science*, 376(6594):eabl5197, 2022.

523 Yin Fang, Xinle Deng, Kangwei Liu, Ningyu Zhang, Jingyang Qian, Penghui Yang, Xiaohui Fan,
524 and Huajun Chen. A multi-modal ai copilot for single-cell analysis with instruction following.
525 *arXiv preprint arXiv:2501.08187*, 2025a.

526 Yin Fang, Qiao Jin, Guangzhi Xiong, Bowen Jin, Xianrui Zhong, Siru Ouyang, Aidong Zhang,
527 Jiawei Han, and Zhiyong Lu. Cell-o1: Training llms to solve single-cell reasoning puzzles with
528 reinforcement learning. *arXiv preprint arXiv:2506.02911*, 2025b.

529 Minsheng Hao, Jing Gong, Xin Zeng, Chiming Liu, Yucheng Guo, Xingyi Cheng, Taifeng Wang,
530 Jianzhu Ma, Xuegong Zhang, and Le Song. Large-scale foundation model on single-cell tran-
531 scriptomics. *Nature Methods*, pp. 1–11, 2024.

532 Shuai He, Lin-He Wang, Yang Liu, Yi-Qi Li, Hai-Tian Chen, Jing-Hong Xu, Wan Peng, Guo-Wang
533 Lin, Pan-Pan Wei, Bo Li, et al. Single-cell transcriptome profiling of an adult human cell atlas of
534 15 major organs. *Genome biology*, 21:1–34, 2020.

535 Ana-Maria Istrate, Fausto Milletari, Fabrizio Castrotorres, Jakub M Tomeczak, Michaela Torkar,
536 Donghui Li, and Theofanis Karaletsos. rbio1-training scientific reasoning llms with biological
537 world models as soft verifiers. *bioRxiv*, pp. 2025–08, 2025.

540 Harrison Lee, Samrat Phatale, Hassan Mansoor, Kellie Ren Lu, Thomas Mesnard, Johan Ferret,
 541 Colton Bishop, Ethan Hall, Victor Carbune, and Abhinav Rastogi. Rlaif: Scaling reinforcement
 542 learning from human feedback with ai feedback. 2023.

543

544 Daniel LeVine, Syed Asad Rizvi, Sacha Lévy, Nazreen Pallikkavaliyaveetil, David Zhang, Xingyu
 545 Chen, Sina Ghadermarzi, Ruiming Wu, Zihe Zheng, Ivan Vrkic, Anna Zhong, Daphne Raskin,
 546 Insu Han, Antonio Henrique de Oliveira Fonseca, Josue Ortega Caro, Amin Karbasi, Rahul Mad-
 547 hav Dhadapkar, and David van Dijk. Cell2sentence: Teaching large language models the language
 548 of biology. In *ICML*. OpenReview.net, 2024.

549 Mohammad Lotfollahi, F Alexander Wolf, and Fabian J Theis. scgen predicts single-cell perturba-
 550 tion responses. *Nature methods*, 16(8):715–721, 2019.

551

552 Erpai Luo, Minsheng Hao, Lei Wei, and Xuegong Zhang. scdiffusion: conditional generation of
 553 high-quality single-cell data using diffusion model. *Bioinformatics*, 40(9):btae518, 2024.

554

555 Sai Ma, Bing Zhang, Lindsay M LaFave, Andrew S Earl, Zachary Chiang, Yan Hu, Jiarui Ding,
 556 Alison Brack, Vinay K Kartha, Tristan Tay, et al. Chromatin potential identified by shared single-
 557 cell profiling of rna and chromatin. *Cell*, 183(4):1103–1116, 2020.

558

559 Nicholas Matsumoto, Hyunjun Choi, Jay Moran, Miguel E Hernandez, Mythreye Venkatesan, Xi Li,
 560 Jui-Hsuan Chang, Paul Wang, and Jason H Moore. Escargot: an ai agent leveraging large language
 561 models, dynamic graph of thoughts, and biomedical knowledge graphs for enhanced reasoning.
Bioinformatics, 41(2):btaf031, 2025.

562

563 Long Ouyang, Jeffrey Wu, Xu Jiang, Diogo Almeida, Carroll L. Wainwright, Pamela Mishkin,
 564 Chong Zhang, Sandhini Agarwal, Katarina Slama, Alex Ray, John Schulman, Jacob Hilton, Fraser
 565 Kelton, Luke Miller, Maddie Simens, Amanda Askell, Peter Welinder, Paul F. Christiano, Jan
 566 Leike, and Ryan Lowe. Training language models to follow instructions with human feedback.
 567 In *NeurIPS*, 2022.

568

569 Rafael Rafailov, Archit Sharma, Eric Mitchell, Christopher D Manning, Stefano Ermon, and Chelsea
 570 Finn. Direct preference optimization: Your language model is secretly a reward model. *Advances
 in neural information processing systems*, 36:53728–53741, 2023.

571

572 Syed Asad Rizvi, Daniel Levine, Aakash Patel, Shiyang Zhang, Eric Wang, Sizhuang He, David
 573 Zhang, Cerise Tang, Zhuoyang Lyu, Rayyan Darji, et al. Scaling large language models for next-
 574 generation single-cell analysis. *bioRxiv*, pp. 2025–04, 2025.

575

576 Åsa Segerstolpe, Athanasia Palasantza, Pernilla Eliasson, Eva-Marie Andersson, Anne-Christine
 577 Andréasson, Xiaoyan Sun, Simone Picelli, Alan Sabirsh, Maryam Clausen, Magnus K Bjursell,
 578 et al. Single-cell transcriptome profiling of human pancreatic islets in health and type 2 diabetes.
Cell metabolism, 24(4):593–607, 2016.

579

580 Zhihong Shao, Peiyi Wang, Qihao Zhu, Runxin Xu, Junxiao Song, Xiao Bi, Haowei Zhang,
 581 Mingchuan Zhang, YK Li, Yang Wu, et al. Deepseekmath: Pushing the limits of mathemati-
 582 cal reasoning in open language models. *arXiv preprint arXiv:2402.03300*, 2024.

583

584 Ankur Sharma, Elaine Yiqun Cao, Vibhor Kumar, Xiaoqian Zhang, Hui Sun Leong, Angeline
 585 Mei Lin Wong, Neeraja Ramakrishnan, Muhammad Hakimullah, Hui Min Vivian Teo, Fui Teen
 586 Chong, et al. Longitudinal single-cell rna sequencing of patient-derived primary cells reveals
 587 drug-induced infidelity in stem cell hierarchy. *Nature communications*, 9(1):4931, 2018.

588

589 Shuaijie She, Yu Bao, Yu Lu, Lu Xu, Tao Li, Wenhao Zhu, Shujian Huang, Shanbo Cheng, Lu Lu,
 590 and Yuxuan Wang. Dupo: Enabling reliable llm self-verification via dual preference optimization.
arXiv preprint arXiv:2508.14460, 2025.

591

592 Sanjay R Srivatsan, José L McFaline-Figueroa, Vijay Ramani, Lauren Saunders, Junyue Cao,
 593 Jonathan Packer, Hannah A Pliner, Dana L Jackson, Riza M Daza, Lena Christiansen, et al. Mas-
 594 sively multiplex chemical transcriptomics at single-cell resolution. *Science*, 367(6473):45–51,
 595 2020.

594 Aravind Subramanian, Rajiv Narayan, Steven M Corsello, David D Peck, Ted E Natoli, Xiaodong
595 Lu, Joshua Gould, John F Davis, Andrew A Tubelli, Jacob K Asiedu, et al. A next generation
596 connectivity map: L1000 platform and the first 1,000,000 profiles. *Cell*, 171(6):1437–1452, 2017.
597

598 Christina V Theodoris, Ling Xiao, Anant Chopra, Mark D Chaffin, Zeina R Al Sayed, Matthew C
599 Hill, Helene Mantineo, Elizabeth M Brydon, Zexian Zeng, X Shirley Liu, et al. Transfer learning
600 enables predictions in network biology. *Nature*, 618(7965):616–624, 2023.

601 Yurong Xin, Jinrang Kim, Haruka Okamoto, Min Ni, Yi Wei, Christina Adler, Andrew J Murphy,
602 George D Yancopoulos, Calvin Lin, and Jesper Gromada. Rna sequencing of single human islet
603 cells reveals type 2 diabetes genes. *Cell metabolism*, 24(4):608–615, 2016.

604
605
606
607
608
609
610
611
612
613
614
615
616
617
618
619
620
621
622
623
624
625
626
627
628
629
630
631
632
633
634
635
636
637
638
639
640
641
642
643
644
645
646
647